DNA Alignment at Cationic Lipid Monolayers at the Air/Water Interface

Christian Symietz, Marc Schneider, Gerald Brezesinski,* and Helmuth Möhwald

Max Planck Institute of Colloids and Interfaces, D-14424 Potsdam, Germany

Received June 20, 2003; Revised Manuscript Received March 10, 2004

ABSTRACT: The interaction of DNA with other DNA and with charged interfaces is of utmost importance for understanding nonviral transfection and DNA diagnostics with optimized chips. This can be studied in detail using Langmuir monolayers of cationic lipids as soft surface of a DNA containing subphase. The positional order of the lipid and the DNA sublattices can be studied by synchrotron X-ray diffraction under continuous variation of parameters such as molecular density or surface pressure. It is shown that DNA binding condenses the membrane surface, and the resulting structure is determined by the interplay of DNA−lipid and DNA−DNA interactions.

Introduction

Research on DNA−lipid interactions is motivated predominantly by two medical applications: (i) There are many expectations on nonviral gene transfer, and DNA complexes with cationic lipids seem to be highly promising candidates.[1−8] (ii) Many diagnostic applications with detection of specific base pairing (lab on the chip) require DNA adsorbed on a surface in a suitable way to be exposed to either complement and/or polymerase.[9−11] Compared with biological methods of gene transfer (like virus application), the use of lipid−DNA complexes is potentially less harmful to the organism.[12] At present, already one-fifth of the clinical trials are performed with these artificially designed complexes, and successful applications are reported not only for cancer and neurological diseases but also for a number of other impairments.[5,13] Yet their cytotoxicity remains to be a problem.[14−16] Moreover, the whole concept depends on overcoming several barriers that significantly limit the efficiency of these new vectors: they have to be able to attach on the target cell, cross the membrane, and release the DNA into the cytoplasm to allow for an entry into the nucleus. The DNA carrier system has to shield the nucleic acid from nuclease or other disintegrating systems. In the cell nucleus, though, the DNA has to be released completely from the surrounding lipids. No gene expression can be observed if one injects lipid−DNA complexes (lipoplexes) directly into the nucleus.[17] Both in vitro and in vivo it was found that positively charged lipoplexes have an increased efficiency for transfection compared to neutral ones. This must be seen in context with the physical stability that depends directly on the lipid composition and the lipid-to-DNA ratio.[5,13] The consciousness for the necessity to design more intricate carrier systems in order to achieve successful transfection is increasing at present.[18]

Along these lines there have been many beautiful experiments illuminating also many exciting general, biophysical, and polymer-physical aspects. Mesoscopic lamellar and hexagonal superlattices of lipids and DNA have been observed by X-ray diffraction with mechanical properties such as smectic alloys.[19−25] A study of liquid-crystalline DNA gel underlined the importance of entropy and an hydration layer (about 3 Å, close to the dimension of one water molecule) in the directly measured interhelical forces.[26] These structures may become interesting materials, but they may probably be too rigid for efficient transfection. However, it may still be interesting to measure their interaction with cell surfaces and membranes to trace their passage into the cell nucleus and their unfolding. Predominantly by scanning force microscopy (AFM), the arrangement of DNA adsorbed to lipid bilayers, which are bound to atomically flat and hard surfaces (mica), has been investigated.[27,28] Parallel arrangement of the polymer strands was observed, but the order extends over merely a few polymer diameters. One reason for this may be that the charge densities of polymer and lipid surfaces do not match at all and that the rigidity of the surface inhibits rearrangements necessary for annealing. Even the binding force of individual DNA molecules to a mica surface could be measured directly with AFM tips.[29] It is possible to confine DNA to artificial microchannels.[30,31]

A further exploitation of these promising applications is hampered by the fact that the interaction of DNA with lipids and with charged interfaces is not well understood. Progress in this direction can be expected by studying a Langmuir monolayer of phospholipids as a model surface in contact with DNA dissolved in the subphase. With this system, the molecular density and thus also the charge density can be varied in a predetermined and continuous way, and the energetics and phase transitions can be studied. This is not possible with DNA coupled to supported bilayers or directly to solid support. The Langmuir monolayer interface is soft, even fluid; i.e., it yields to forces exerted by polyelectrolyte adsorption, which may enable an optimized arrangement. On the other hand, measuring the structural changes effected by adsorption also sheds light into these interactions. The significance of the presented study lies in the technical possibility to change surface properties with purely mechanical means (the barrier of the film balance) and in the chance to study the adsorbed layer in a wide range of pressure and density.

Materials and Methods

Methyltrioctadecylammonium bromide (TODAB), purity >98%, and dimethyldioctadecylammonium bromide (DODAB) were purchased from Fluka (Germany). Both compounds are well soluble in chloroform (Merck, Germany) and were spread with a microliter syringe as 0.5 mM solutions on the subphase. The subphase water was purified with a Millipore filter to a specific resistance of 18.2 MΩ cm. Sodium chloride for the DNA solutions was heated to 600 °C to reduce the content of potential organic impurities.

10.1021/ma0348425 CCC: $27.50
Published on Web 04/22/2004

The double-stranded deoxyribonucleic acid (DNA), purchased from Sigma (Taufkirchen, Germany), is a highly polymerized natural product originating from calf thymus. The preparation (Lowry) yields a DNA sodium salt in the form of a white fibrous substance containing less than 3% of protein. A molecular weight for this Sigma product is reported[32] to be 4.5×10^6 g/mol, which yields an average size per molecule of 6500 base pairs, equal to a length of 2.21 μm. This sample was used without further purification. The experiments do not give rise to suspicion of monolayer damage or disturbances due to protein or other possible impurities. To minimize the danger of DNA denaturation, all experiments have been performed at 20 °C, and only fresh solutions of DNA were used that contained 1 mM NaCl. The salt solution was prepared before the DNA was added to the flask. After 2 h of using a magnetic stirrer at 20 °C, the DNA was completely dissolved.

The pressure/area isotherms were measured with a Wilhelmy system in a Langmuir trough (Riegler & Kirstein, Germany). A thermostate kept the temperature at 20 °C, and the surface pressure was recorded during the monolayer compression.

If the lipid density varies at the water surface and areas with different refractive indices form, one can detect these inhomogeneities with a Brewster angle microscope (BAM). The intensity of the reflected polarized light depends on the refractive index of the reflecting material. Domains of higher molecular densities can be seen as brighter areas compared to the dark background when observing the water surface under the Brewster angle. The light of a diode laser is detected with a CCD camera, both being parts of a commercial microscope (BAM2, Nanofilm Technology Ltd., Göttingen, Germany) mounted on a Teflon trough for film characterization. The images are recorded on videotape, analyzed with software, and corrected for the perspective of observation under an oblique angle. The spatial resolution is about 2 μm.

Another method of direct and video-based observation of a monolayer at the air/water interface is fluorescence microscopy. The resolution ($\sim$1 μm) of the images is typically better than with Brewster angle microscopy. Contrast in the pictures originates from the different solubilities of added fluorescent dye in coexisting phases of the monolayer. Not more than 2 mol % of a dye should be used. We added 2 mol % of 2-(12-(7-*N*-nitrobenz-2-oxa-1,3-diazol-4-yl)amino)dodecanoyl-1-hexadecanoyl-*sn*-glycero-3-phosphocholine (NBD-C_{12}-HPC) to the chloroform solution of TODAB. This did not change the pressure−area isotherm compared to the measurements without the dye. A microscope (Zeiss, Axiotron) was mounted above a translational *xy* stage that could move the trough (Riegler & Kirstein, Germany) horizontally below the microscope objective. A 50 W Hg lamp combined with optical filters illuminated the sample in a wavelength region around the absorption maximum of the dye. Another filter allowed the fluorescence light to pass through the microscope into a highly sensitive SIT camera (Hamamatsu C2400). The picture could simultaneously be observed on a monitor during the experiment.

With a scanning force microscope (D3000, Digital Instruments, Santa Barbara, CA) we mapped the hydrophilic surface of TODAB/DNA monolayers. The coupled layer of TODAB and DNA was compressed to 25 or 42 mN/m. A silicon wafer was made hydrophobic with a surface layer of OTS (octadecyltrichlorsilane, $CH_3(CH_2)_{17}SiCl_3$) and was lowered with a motor driven dipping device to touch the monolayer surface. The wafer was oriented parallel to the water surface, a method called the Schaefer technique. As soon as it was completely wetted on its lower side, the sample was lifted up again, remaining wet. This gives rise to the assumption that it has been completely covered with the TODAB hydrocarbon chains attached to the wafer and the DNA molecules remaining at the now hydrophilic surface. It was immediately immersed into a self-made Teflon fluid cell filled with pure water. The scanning was done in water with rectangular SiO_2 AFM cantilevers (Silicon-MDT, Russia) with typical force constants of approximately 0.6 N/m. The pictures were recorded using the tapping mode.

X-ray diffraction was performed at HASYLAB, DESY in Hamburg, Germany. The undulator beamline BW1[33] of the synchrotron is equipped with a liquid surface diffractometer, allowing grazing incidence diffraction (GID) on monolayers at the air−water interface.[34] A monochromatic beam ($\lambda = 1.304$ Å) from a beryllium crystal strikes the water surface at an angle of 0.11°, equal to 85% of the critical angle of total external reflection of water for this X-ray wavelength. The area of the monolayer illuminated by the incoming beam is close to one square centimeter (2×50 mm^2). This size allows a comparison of the X-ray data with the optical microscopy results because it includes and averages over all inhomogeneities, which are visible with microscopical techniques (on the order of micrometers). A linear position-sensitive detector (PSD) (Braun, Garching, Germany) measures the vertical intensity distribution of the scattered signal. A Soller collimator made of vertically oriented parallel plates positioned in front of the PSD defines the resolution in the horizontal direction 2θ.

The scattering vector **Q** can be decomposed into a horizontal component $Q_{xy} \approx (4\pi/\lambda) \sin(2\theta/2)$ and a vertical component $Q_z \approx (2\pi/\lambda) \sin(\alpha_f)$, with α_f being the vertical scattering angle. The accumulated position-resolved counts were corrected for polarization, effective area, and Lorentz factor. Model peaks taken as a Lorentzian in the in-plane direction and a Gaussian in the out-of-plane direction were least-squares fitted to the measured intensities. In general, lipid monolayers can be treated as 2D powders, namely, 2D crystals oriented in random directions in the monolayer plane. From the peak positions of the horizontal (in-plane) diffraction data, the lattice spacing can be determined as $d = 2\pi/Q_{xy}$, where Q_{xy} is the maximum of the Lorentz curve. From this, the lattice parameters a, b, and γ can be calculated, giving the unit cell area A_{xy}. For the hydrocarbon chains of the lipids this is the projection of the chain cross-section area $A_0 = A_{xy} \cos(t)$ onto the horizontal plane. The tilt angle t is the angle between the normal of the water surface and the symmetry axis of the hydrocarbon chain. It is zero (untilted chains) if there are diffraction peaks only at zero Q_z. An undistorted hexagonal lattice exhibits a single diffraction peak. Two diffraction maxima occur for a centered rectangular lattice where the chain tilt may be directed toward the nearest neighbor (NN) or the next-nearest neighbor (NNN). Three nondegenerate diffraction peaks originate from an oblique chain lattice with three different spacings.

The peak profile in Q_{xy} direction allows the calculation of the positional correlation length ξ, giving an estimation for the size of the laterally ordered crystallites in the monolayer. If the correlation at their edges decays exponentially, the resolution corrected full width at half-maximum (fwhm) ΔQ_{xy} gives $\xi = 2/\Delta Q_{xy}$. This is the case for diffraction peaks with a Lorentz profile that could be applied to all measurements with our samples. In the case of Gaussian profiles, the crystallites would be perfectly ordered up to the edge and the Scherrer equation would hold: $\xi = 5.53/\Delta Q_{xy}$.

Results and Discussion

Experiments were performed using the triple-chain lipid TODAB and the double-chain lipid DODAB. The more outstanding results, presented here, were obtained with TODAB, whereas data on the other system are used for comparison.

A concentration of 0.1 mM was used for the DNA solutions in most experiments. If it was 10 times higher or lower, no different results were obtained for the isotherms or X-ray diffraction measurements. In the diagrams we present data of the more pronounced X-ray peaks of experiments with 1 mM DNA solutions. The concentration refers to a DNA monomer = nucleic acid + helix element (sugar phosphate backbone) containing one charge or counterion after dissociation in water. The dominating force for the DNA binding to the lipid is electrostatic attraction. To estimate the amount neces-

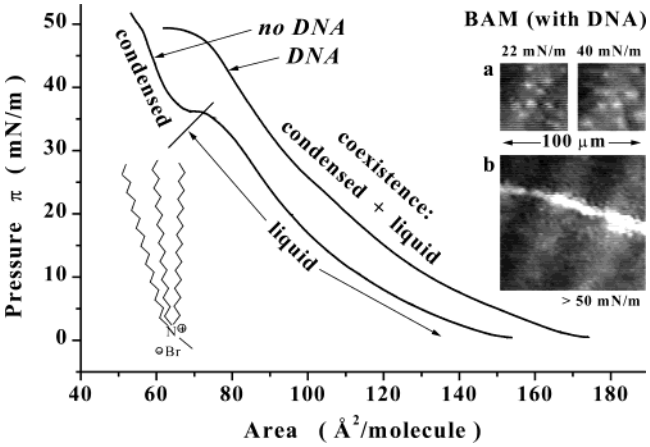

Figure 1. Pressure/area isotherms of TODAB on pure water (left curve) and on a 1 mM solution of DNA (right curve) measured at 20 °C. The area per molecule in both cases refers to the TODAB molecules alone, not including DNA. A small plateau near 35 mN/m (transition region between the liquid and condensed phases) can be seen on water. The chemical structure of TODAB is shown in the ionized form. The BAM pictures (all in the same scale) present an inhomogeneous layer both below (a) and above (b) the collapse pressure. The collapse structure (white line) coexists with remaining irregularities of the film. Therefore, the darker parts are not purely liquid surface areas. The lines of changing brightness perpendicular to the collapse structure are interference patterns that do not originate from the monolayer.

sary to obtain a close DNA packing at the interface, the amount of a purely hypothetical parallel alignment with an interhelical distance of 20 Å was calculated. This corresponds to 20 possible DNA layers per millimeter depth of the 0.1 mM solution (or 200 layers/mm for 1 mM). Time-dependent measurements of the surface pressure were conducted after spreading TODAB onto the DNA solution to reach a starting pressure of 8 mN/m. Adsorption of DNA from the subphase leads to a final pressure of 12 mN/m after only a few minutes, showing that 20 min is enough time for an adsorption layer to form at the surface. The concentration of DNA in the solutions was high enough to assume a time interval of the order of seconds that ensures the diffusion of enough DNA for charge compensation to bind to the lipid layer. Already 30 min after spreading the lipid layer onto the DNA solution, we found intense X-ray scattering signals: The DNA had not only adsorbed but also arranged parallel to the surface, even before any layer compression has been started. The liquidlike compressibility of the coupled TODAB/DNA layers and the stable profile of the X-ray peaks make us believe that all measurements were performed close to equilibrium. Any long-term changes are likely to be of minor significance and were no subject of the presented study.

Figure 1 presents pressure/area isotherms of a TODAB monolayer in the absence and in the presence of DNA in the subphase. In the absence of DNA, one observes a change in slope near 35 mN/m, corresponding to a phase transition from a fluid to an ordered phase. In this plateau region one could expect to find a heterogeneous TODAB structure. However, it was not observed with Brewster angle and fluorescence microscopy presumably because the size of condensed domains was below the spatial resolution. With DNA in the subphase, the film is more expanded (DNA adsorbs to and penetrates into the monolayer) and the phase transition disappears (strong electrostatic coupling of lipids to DNA; no uncoupled lipids, which can undergo the phase transition observed in the pure lipid film). Yet the liquidlike compressibility of the film does not mean that it corresponds to a completely disordered state. On the contrary, we will show below that even at low pressure (10 mN/m) one observes an ordered lipid phase, but with a density a factor of 2 smaller than given by the isotherm. This means that the film is heterogeneous, and only at higher pressure above 20 mN/m can one observe these heterogeneities by Brewster angle microscopy (BAM) (Figure 1a). The islands correspond to an ordered state, the continuous phase (dark background in the BAM pictures) being presumably DNA at the interface perhaps with some lipid attached to it. With rising pressure these islands did not disappear but were visible together with collapse structures (linear areas of high reflectivity with lengths in the range of several millimeters) above 50 mN/m (Figure 1b). The brighter domains were at no pressure surrounded by a completely liquid phase of pure TODAB which follows from: (a) the lack of a plateau region in the pressure−area isotherm (coexistence of liquid and condensed phases with lower compressibility relative to the neighboring parts of the pressure/area isotherm) and (b) the BAM observation that the domains did not move relative to each other. Two different kinds of condensed or relatively stiff parts of the monolayer existed that blended into each other, showing no defined boundaries at the edges of the domains.

It should be mentioned that we observed no DNA adsorption to the water surface in absence of the lipid: There was no X-ray scattering even after more than 1 h of waiting time. Nonordered DNA, though, would not result in a peak, but it would increase the surface pressure, an effect that has not been observed either. Thus, we believe that some DNA coupled to the lipid layer and induced the lattice structure of the lipid described below. Another part of the water surface consisted of a lipid/DNA layer that did not result in an X-ray signal and therefore must have been in a disordered state for both the lipid and the DNA. This part is represented by the darker areas in the BAM pictures. Either only lipid or only DNA existing in the dark part of the surface is extremely unlikely because TODAB alone would be fluid and must be compressible, forming a homogeneous layer at least at high pressures. So it should contain at least some DNA because of the suppressed fluidity of the film as observed with BAM, and additionally some TODAB must have been present at the surface because without the lipid the DNA would have remained in solution instead of binding to the interface.

Fluorescence microscopy shows that the pure TODAB layer looks homogeneous even at 5 °C, where the two-phase coexistence plateau appears at 8 mN/m instead at 35 mN/m observed at 20 °C. However, in the presence of DNA, some structures were big enough to appear as dark (molecularly ordered) spots at pressures above 10 mN/m (Figure 2). They began to form around central cores with up to a few hundred micrometers in diameter and were surrounded by other much smaller spots whose size decreased with increasing distance from the central region. They increased in number and size with compression of the monolayer. In accordance with the BAM measurements, the whole surface seemed to have such a high viscosity that no relative movement of domains was observed. Immediately after spreading TODAB onto the DNA-containing subphase, one could

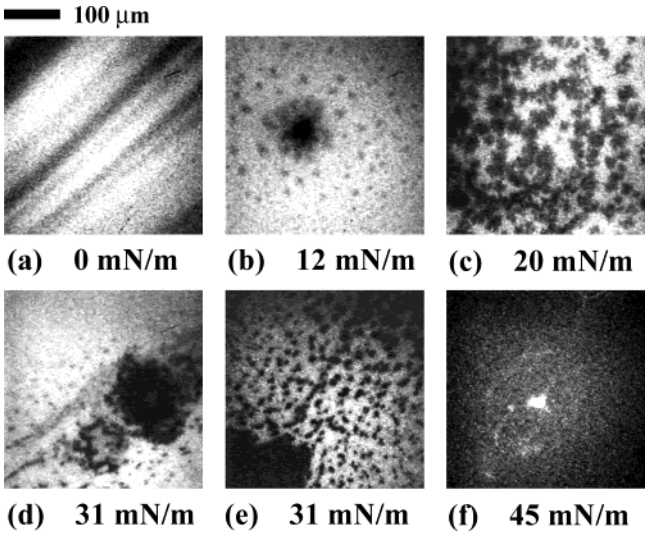

Figure 2. Fluorescence microscopy pictures of TODAB on a 0.1 mM DNA solution at different surface pressures and 20 °C: (a) linear structures visible during the spreading process of the lipid, that do not dissolve completely; (b−e) formation of dark, condensed spots during the compression of the monolayer; (d) and (e) show a stable, underlying linear structure like the one observed during the spreading together with condensed spots; (f) during or after the collapse of the layer, locally higher concentration of the fluorescent marker surrounded by a still inhomogeneous surface (better visible by direct observation). The scale is the same for all pictures.

observe some long linear features: areas slightly darker than the rest of the surface, stretching out over the range of millimeters (Figure 2a). They were not observed with TODAB on pure water. These hazy areas were visible at all pressures (Figure 2d,e), seemed to be quite stable, and gave the impression of a limited fluidity, thus allowing the assumption that a fast adsorption of DNA to the lipid during the process of spreading avoids the formation of a completely homogeneous TODAB layer even before the compression. If the lipid layer (TODAB + fluorescent dye) was liquid, one must expect completely homogeneous fluorescence intensity. Although the reason for the inhomogeneities is not certain, it is an argument in favor of a suppressed or at least drastically reduced lateral diffusion of the lipids in the presence of DNA. It is very likely that DNA adsorbed everywhere at the surface but condensed together with TODAB only locally, leaving the major part in a less dense and less ordered state.

To reduce the risk of induced disorder due to a layer transfer onto a solid support, we have performed AFM measurements in water, not in air. A hydrophobic silicon wafer touching the monolayer with the flat side (parallel to the water surface) was used, thus ruling out any defect that could originate from vertical dipping techniques (drainage of water). After the flat side of the wafer had contact with the water, it was pulled up immediately, now being covered completely with a water layer, showing that a coupled TODAB/DNA layer was transferred. To prevent it from drying, it was immersed into water right after the transfer. Ample care was taken to keep the sample hydrated. However, some kind of transfer artifact is unavoidable. Analysis of the pictures allowed to identify two main levels of the samples: an average background and above it a distribution of matter that had an average thickness relative to the background of 40 ± 10 Å. The transition from the lower to the higher level was not steep and represented the true surface with a high probability. Typical AFM tips with radii of <100 Å easily resolve the surface in such a slope region. A calculation of the artificial increase at the edge of sample steps due to the tip geometry[35] shows that only much larger tips with a radius of more than 1000 Å would produce this observed step profile, which therefore was not a result of limited resolution. The layer transferred at 25 mN/m gave images that showed islands from almost round to elongated shape with a maximum ratio of big to small diameter of about two. The smaller one was roughly 700 Å. Only few of these features fused partly, leaving the wafer homogeneously covered with spots (between 60 and 70% of the surface area). The layer prepared at 42 mN/m did not differ in thickness, but the pattern is of different quality: The islands seemed to have fused so much as to leave a spongelike distribution of a plateau filled with holes, still in a similar area ratio of thick to thin as at 25 mN/m. The average distance between the holes in the layer (about 2000 Å) shows that the size of the fused material has increased. If or how much these structures were induced by the transfer to and the contact with the hydrophobic wafer is an open question. Nevertheless, it followed from the X-ray diffraction of the layer on water (as well as the BAM and fluorescence microscopy) that there must have been some kind of inhomogeneity. This will be shown below. The surface of the silanized silicon wafer is a densely packed arrangement of hydrocarbon chains in contact with the hydrocarbon chains of the TODAB molecules. The attracting van der Waals forces between these two hydrocarbon chain layers are typically sufficient to guarantee a stable film transfer. There is no reason for the TODAB chains to rearrange at the homogeneous and flat surface of hydrocarbon chains in contrast to monolayers that are transferred the other way round: charged or polar headgroups are more likely to react to charge distributions on solid wafers, resulting in rearranged layers with sometimes strongly altered densities. So far we can assume that the features observed with AFM do not have their origin in the transfer process. Force microscopy under water did not offer the spatial resolution that would have been necessary to prove that the highest level of matter in the pictures was DNA; the molecular ordering was below that resolution and could not be seen. We assume that the two main levels represent a TODAB layer together with some disordered DNA as the background and above the DNA in a densely packed arrangement. The possibility should not be ruled out that the lower background level were just holes in the transferred layer caused by a lipid concentration which was locally too low for a good film transfer to the wafer, but there is no further experimental evidence supporting this idea. After the following presentation of the X-ray diffraction results, a discussion will bring more insight into the ever-present inhomogeneities of the TODAB/DNA layer.

The GIXD data are in accordance with the pressure/area isotherm of pure TODAB on water (without DNA). At pressures below the transition around 35 mN/m no diffraction peak of condensed material was visible, but some signal was there originating from the hydrocarbon chains of the lipid in the liquidlike state. This halo with low intensity shows that only very few molecules or even single molecules contribute to the X-ray signal (lateral correlation length of less than 30 Å). Such a signal of lipid chains in the liquid-expanded phase was not

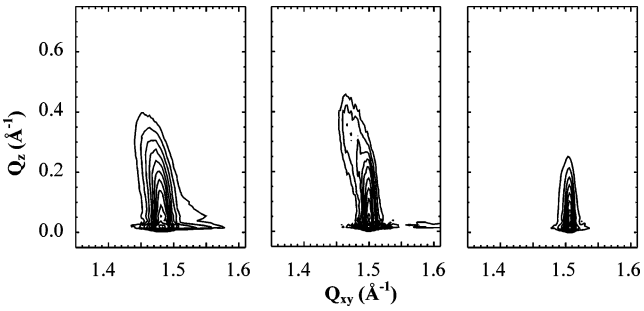

Figure 3. Contour plots of the corrected X-ray intensity vs in-plane and out-of-plane scattering vector components Q_{xy} and Q_z, respectively, of a TODAB monolayer. $Q_z = 0$ corresponds to the water surface. At $\pi = 45$ mN/m, TODAB on pure water (left) forms a centered rectangular lattice of tilted ($t = 13°$) hydrocarbon chains. After coupling of DNA, a condensed chain lattice with $t = 14°$ appears already at 10 mN/m (middle), and at 20 mN/m (right) the untilted chains are packed in a hexagonal lattice.

observed with single- or double-chain molecules. Maybe the three chains attached to the nitrogen of one TODAB molecule are packed densely enough to produce the observed halo. This opinion was supported by the observation of an even more prominent halo in the liquid-expanded phase of the four-chain anionic phospholipid tetramyristoylcardiolipin (Avanti Polar Lipids). There was no gradual transition from the halo signal of the liquid TODAB to the pronounced peak of the condensed monolayer. It appeared above the pressure of the phase transition. A detailed analysis of the distribution of the diffracted intensity (contour plot in Figure 3) indicates a uniform tilt of the aliphatic tails of $t = 13°$ at 45 mN/m. The two-dimensional lattice is rectangular, and the chains are tilted in the NN direction. Comparing the area per molecule, derived from the isotherm (about 60 Å^2 per molecule above the plateau region), with the in-plane area per chain (21.3 Å^2), calculated from the X-ray data, shows that the TODAB layer is homogeneous. This is also in agreement with both the BAM and the fluorescent microscopy pictures that showed only a homogeneous brightness throughout the whole picture in every phase of the lipid.

The adsorption of DNA from the subphase to the lipid layer had a strong influence on its phase behavior and structure. A tendency was observed toward a condensation of TODAB. Although the results differ slightly in repeated experiments, the scattering of data was still limited enough to distinguish clearly from the measurements on pure water. The limited reproducibility might have its origin in a possible fast adsorption of DNA during the spreading of the TODAB solution, in accordance with the fluorescence microscopy measurements described above. In presence of DNA, the common feature of the diffraction experiments was the observation of NN-tilted TODAB chains at pressures below the phase transition on water and a phase transition into a nontilted state on compression, which was never observed on pure water. At 3 mN/m, a rectangular TODAB chain lattice with a uniform NN tilt of 19° was observed due to the coupling of DNA. The area per TODAB molecule, derived from the pressure/area isotherm, amounts to 150 Å^2. This area is more than twice as big as tightly packed TODAB molecules required: The GID data resulted in 21.4 Å^2 for each hydrocarbon chain (about 64 Å^2 per molecule). With compression, the tilt angle was reduced to 14° (at 10 mN/m) and finally to 0° at 20 mN/m (with 60.3 Å^2 per molecule) (Figure 3). The in-plane correlation lengths, derived from the fwhm of the diffraction peaks, were around 70 Å in the absence of DNA. In the presence of DNA they were increased to 180 Å and again reduced at high pressure (30 Å). This behavior was not observed for lipids in the absence of polymers in the subphase where compression leads to a narrowing of diffraction peaks. Both the reduced tilt angle of the hydrocarbon chains and the increased correlation length of the lipid lattice underline the active role of DNA to condense the TODAB monolayer.

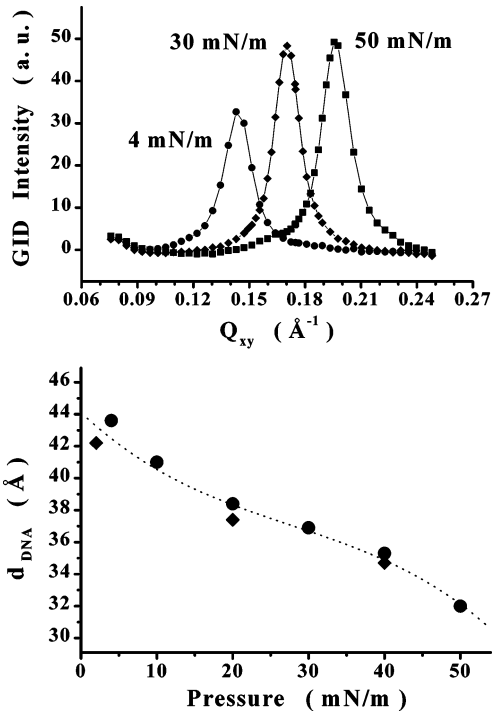

Figure 4. Background subtracted diffraction peaks (upper picture) of aligned DNA. The peak shifts toward larger Q_{xy} values during monolayer compression (surface pressure indicated next to the peaks). The corresponding lattice spacing between the DNA chains d_{DNA} as a function of the surface pressure π is shown in the diagram below. The round symbol (●) belongs to the peaks in the diagram above, and the other data points (◆) refer to other measurements showing the same compression behavior. The dotted line through the data points is not a fit but simply to guide the eye.

The most exciting and unexpected finding of this work was the observation of diffraction peaks ascribable to DNA ordering (Figure 4). With compression, these peaks shifted to lower spacings and the half-width decreased by a factor of 2.5 and passed through a minimum at 30 mN/m. Likewise, the integrated intensity increased by a factor of 3, exhibiting a maximum at 30 mN/m. Thus, the packing had an optimum at a pressure much below the collapse at 50 mN/m. The lateral ordering of DNA must be a result of a compromise: The attraction to the lipid (charge compensation) and the opposing repulsion of the DNA chains (electrostatics and thermal energy). The reproducibility of the DNA spacing was limited to an interval of about ±4 Å for each pressure. This scattering was independent of the DNA concentrations used (0.01, 0.1, and 1 mM). Nevertheless, the compressibility of the different DNA layers was the same for repeated experiments: Plotting the Q value as a function of lateral pressure (not shown here) gives $dQ/d\pi = (9 \pm 1) \times 10^9$ N^{-1}. The absolute value of d_{DNA} for a given surface pressure depended on some hitherto unknown condition in the layer preparation or spreading process.

The differences between the measurement may arise from the fact that the lipid solution was spread onto the DNA subphase: The dropwise spreading procedure lasts 1−2 min. During this time DNA starts to adsorb, producing an inhomogeneous layer with an already decreased fluidity. Compared to experiments with supported bilayers, the monolayers are in a much more expanded state. The observed constant compressibility showed that the individual layers had the same characteristic structure. In other words, TODAB/DNA layers with the same DNA spacing do not need to have the same surface pressure but behave similarly in respect to compression and expansion. Interestingly, the distance between the DNA molecules increased to a value close to the original one at low pressures when the barrier of the film balance moved back to allow a slow expansion of the monolayer. A second compression leads again to decreasing DNA spacing. This reversibility shows that the coupled layers were quite flexible which corresponds well with the fluidlike compressibility (similar to TODAB on water without DNA) even at high pressures.

It is a surprising and remarkable fact that the DNA helices arranged in a one-dimensional lattice even without compression of the monolayer. After spreading the lipid solution and waiting for half an hour, a clear GID signal with low intensity proofs this self-alignment with helix distances between 43 and 49 Å. The intensity of the X-ray signal increases during compression parallel to the portion of ordered DNA, reducing the spacing to about 32 Å at 50 mN/m (Figure 4). In some cases, such clear signals could not be found at low pressure, but the compressed layers always gave very intense X-ray peaks, though with different DNA spacings. Even two separate peaks could be distinguished in some cases close to the collapse pressure, meaning that two different DNA lattices could coexist. The maximum of the Bragg rod was always at zero Q_z. The interpretation of the fwhm of the rods remains to be challenging because it decreases significantly with compression of the layer. Since the peaks arise only from the ordered areas of DNA, one must conclude that compression increases the thickness of the adsorbed DNA layer. One possible calculation of the thickness T from the fwhm ΔQ_z ($T = 5.53/\Delta Q_z$) would result in thickness of DNA layers between 30 Å at low pressure up to almost 70 Å at high pressure. Simultaneously, knowing the lateral spacing between the DNA helices this gives an adsorbed layer with more than 3 times the amount of DNA necessary for complete lipid charge compensation. There is no obvious reason for such a large amount of DNA, thus the interpretation of the line profile in the z-direction is still open.

Calculating the two-dimensional charge density σ_{DNA} = (20 e^-/34 Å d_{DNA}) for DNA with 20 elementary charges per helical turn over the corresponding length of 34 Å leads to values between 1 e^-/83 Å^2 at the lowest pressures and 1 e^-/54 Å^2 for the highest pressure. The lipid charge density σ_L of TODAB cannot be higher than 1 e^-/60.3 Å^2 as observed for the hexagonal chain packing of TODAB coupled to DNA. Taking this as a maximum for the lipid, it could be compensated ($\sigma_{DNA} = \sigma_L$) by DNA in a lateral repeat distance of $d_{DNA} = 35.5$ Å. This lies between the lowest and highest values observed for DNA. Figure 5 shows this correlation: the area per elementary charge (inverse to the charge density) presented vs the surface pressure. Thus, charge compensation alone does not explain the denser packing of DNA at high pressure. The charge densities are calculated for the complete double helix. One should bear in mind that the negative charges are close to the surface of the molecule, so that a significant part of them is up to 20 Å away from the lipid headgroups. Consequently, the effective charge density of DNA, with an influence on the lipid arrangement, should be considered to be smaller. This can be an explanation for the apparent charge overcompensation. The complex interplay of normal (DNA−lipid) and lateral (DNA−DNA) interactions is also influenced by the presence of counterions that possibly shield the charges from each other and allow a small distance between the DNA strands. No direct geometric connection could be found between the hexagonal lipid chain packing with its possible charge distributions and the arrangement of the opposite charges around the helix of the DNA. The attraction between TODAB and DNA might be of unspecific, not pointwise, character; the parallel arrangement of the polymer is not a direct result of the lipid lattice. No matching of charges could be deduced from the calculated lattices. This geometric mismatch can possibly be further stabilized by the entropic contribution of counterion release.

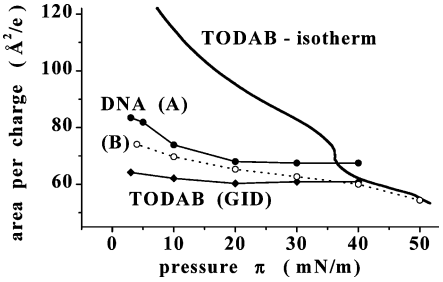

Figure 5. Area per elementary charge (Å^2/e) as a function of surface pressure π. The TODAB pressure/area isotherm (thick line) underlines the extent of local lipid condensation (inhomogeneous layer), when being compared with the GID data of the chain lattice (close to 60 Å^2/e). At low pressures, the average area from the isotherm is more than twice the condensed area of TODAB. Two examples of DNA (calculated area per phosphate group from the measured DNA spacing) illustrate the discrepancy to the lipid. Version (A) indicates no match of charges, whereas (B) shows that compression can even lead to overcompensation of charge densities.

The presence of sodium chloride was necessary to reduce the probability of DNA denaturation. GID was also performed without salt for comparison, but the results did not differ from those with 1 or 10 mM NaCl. So far we have not performed a systematic study about the dependence of the DNA spacing on the salt concentration. Theoretically, we should expect a suppression of DNA adsorption above a critical salt concentration.[32,36,37] In accordance with these calculations, we observed no DNA peak and therefore no ordered adsorption with 1 M NaCl in the subphase, not even 4 h after the TODAB monolayer was prepared. Only slightly higher background intensity was found in the angular range where the DNA signal appeared in the cases of lower salt content. This additional scattering can only be explained by the presence of some disordered DNA near the water surface. It was impossible to induce a parallel alignment of DNA with compression. The behavior of the lipid though was almost like on pure water. A rectangular chain lattice appears already at 30 mN/m, and the lipid molecules remain tilted even at 40 mN/m. This shows that a salt concentration above a

critical value can prevent the formation of a stiff and ordered DNA lattice, although some DNA can adsorb irregularly. To prove the relation between the salt content and a lack of order, the influence of salt addition to an existing ordered DNA layer was determined. DNA was coupled to a TODAB monolayer, giving a distinct X-ray signal. After compression to 50 mN/m and following expansion to 30 mN/m, 5 mL of sodium chloride solution (c = 2 M) was injected under the DNA layer near the footprint area of the X-ray beam. Although the local NaCl concentration is unknown, repeated measurements of the DNA signal revealed a destruction of the two-dimensional lattice or a partial DNA desorption. Two hours after the injection, the DNA peak disappeared into a broad background signal of increased intensity, indicating the presence of disordered DNA. Obviously, a reduced DNA/lipid attraction led to a loss of order or even desorption of the DNA. A recompression of the monolayer to 50 mN/m caused the appearance of two low-intensity peaks belonging to DNA spacings of 37 and 29 Å. Since the injection resulted in badly defined and not reproducible conditions concerning the salt concentration at the surface, no explanation can be given for the simultaneous existence of two different DNA lattices. The experiment could only prove that salt strongly influences the order of adsorbed DNA. Apparently, the Coulomb attraction to the surface is reduced and the repulsion of the charged DNA rods can be partly screened via additional salt in the solution, allowing tighter packing. So far we have not observed a systematic reduction of the interhelical distance due to screening effects; more experiments on this topic are in progress. Fang and Yang[28] observed some DNA ordering on supported bilayers even with 1 M NaCl in the solution. Their results are based on a Fourier transform of AFM pictures, giving an increased value for the inter-DNA distance. We cannot rule out that such a packing also exists at monolayers, but the DNA molecules may not be stretched straight enough in the presence of 1 M NaCl to result in a defined X-ray signal. Fang and Yang explain the increased average DNA distance with a cloud of nonlocalized Na^+ ions condensed onto the DNA rods. These different results cannot be correlated in a direct way since different lipids were used, being in different thermodynamic phases and having unequal charge densities during the adsorption process.

The use of the double-chain lipid DODAB allowed a comparison with the more spacious triple-chain TODAB. A condensed DODAB layer with its higher charge density offers the possibility of tighter DNA packing. This expectation was only partly fulfilled. The pressure/area isotherm on water (not shown here) is characterized by a plateaulike region around 15 mN/m. At this pressure, a weak GID signal indicates the beginning of lipid condensation. At 35 mN/m, the hydrocarbon chains are still tilted with t = 39°. An analysis of the GID data yielded a cross section of the chains of A_0 = 19.9 Å^2. Its projection onto the horizontal plane A_{xy} = 25.6 Å^2 results in a two-dimensional lipid charge density of σ_L = 1 e$^-$/51.2 Å^2. The DODAB layer on pure water is homogeneous because the area per molecule from GID agrees well with the value from the pressure/area isotherm. With DNA in the subphase, a total charge compensation ($\sigma_{DNA} = \sigma_L$) could geometrically be achieved for a DNA packing with d_{DNA} = 30.1 Å. The observed value of 37.2 Å (at π = 40 mN/m) corresponds to σ_{DNA} = 1 e$^-$/63.2 Å^2. The DNA layer could not be compressed so far as to compensate the theoretical lipid charge density. A low-intensity GID signal from the lipid chains coupled to DNA allows the estimation that the charge density of the coupled lipid lies near σ_L = 1 e$^-$/58 Å^2, a value between the one of the lipid on water and the one of DNA ($\sigma_{L,\text{on water}} > \sigma_{L,\text{on DNA}} > \sigma_{DNA}$). Thus, the DODAB monolayer was expanded in the presence of DNA. The low density of DNA packing is in contrast to DNA coupled with TODAB that could be compressed to distances smaller than only charge density arguments would allow. The pressure/area isotherm of DODAB coupled to DNA is expanded even more (plus 40% relative to DODAB on pure water) than in the case of TODAB (plus 20%), but both monolayers exhibit a fluidlike compressibility and do not show any phase transitions.

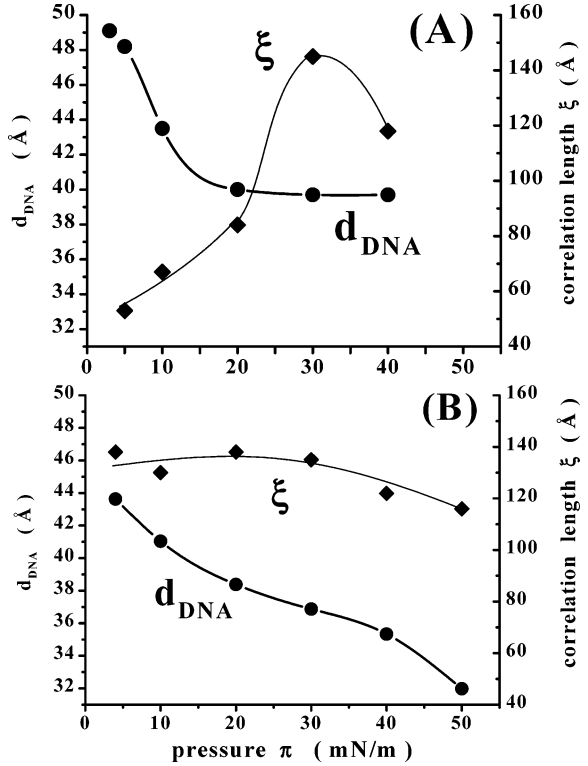

Figure 6. Two extreme examples of DNA coupled with a TODAB monolayer. Each diagram shows the DNA spacing d_{DNA} (●) and the correlation length ξ (◆) of the lateral order of DNA chains as a function of surface pressure π. Example (A) begins with large DNA spacing, which remains constant above 20 mN/m. The corresponding TODAB layer is strongly condensed (see text). The other example (B) shows a densely packed DNA lattice with decreasing d_{DNA} until the collapse. TODAB is condensed only at higher pressures. Common to both examples is a decay of the order of the DNA and TODAB lattices above 30 mN/m. For a better comparison, the diagrams have the same scale.

Summarizing the coupling of DNA to both lipids, DODAB forms a layer with DNA that increases its order during the compression all the way up to the collapse pressure. It is characterized by a strong increase of the peak intensity, indicating an increased amount of aligned DNA. It could not be damaged by monolayer compression, whereas DNA coupled to TODAB exhibits the best alignment near 30 mN/m, far from the collapse. Figure 6 shows the spacing d_{DNA} of DNA coupled to TODAB and the lateral correlation length ξ of DNA in dependence on the surface pressure π for two extreme examples. The calculated values of ξ are only an approximation because the line profile of the scattered

signal is close to but not in perfect agreement with a Lorentz profile. Salditt et al.[22] have made a detailed line shape analysis of their lamellar system with DNA and conclude that the profile is not Lorentzian. Also, in our measurements the DNA lattice is not limited at the edges in a well-determined way (a soft two-dimensional nematic), and the correlation lengths only give one possible answer to the question of domain size. Nevertheless, the restriction to only one definition allows a description of the relative changes of the lattice size, which is directly correlated to the change in line width. Figure 6 illustrates the variability of possible conformations: The properties of the DNA layer and the order of the coupled TODAB seem to depend on the starting condition. Example A is described by less dense initial DNA packing at low pressures, when compared with example B. Above 20 mN/m the spacing remains constant. The corresponding TODAB lattice is locally condensed at low pressure (rectangular lattice of tilted chains already at 3 mN/m) and forms a hexagonal lattice already at 20 mN/m. Both correlation lengths reach a maximum value: 180 Å for TODAB at 20 mN/m and 145 Å for DNA at 30 mN/m. The decrease of the correlation lengths and peak intensities point to the destruction of the lattices with ongoing compression, being even more pronounced for the lipid. Example B begins with a considerably smaller DNA spacing, which decreases all the way up to the collapse. No lipid lattice is observed at the beginning; an untilted phase suddenly appears at 30 mN/m with a lipid correlation length of 138 Å. This equals exactly the size of the DNA ordering which remained constant between 4 and 30 mN/m. This size agreement is a good argument for the assumption that both ordered phases coexist coupled to each other and are not laterally separated. Further compression reduces the DNA correlation length only by 20%, whereas the TODAB domain size shrinks drastically down to only 30 Å. Simultaneously, the hexagonal order is lost and the chains start to tilt. So either lipid or DNA molecules are well-ordered at the beginning, not both simultaneously. Compression improves the packing of both components only to medium pressures, and it was a common feature of the TODAB/DNA layers, also in other measurements, that the size of the ordered DNA domains could not be increased with compression above 30 mN/m. The TODAB lattice reacts even stronger and is destroyed to a higher extent.

Before discussing a model of the lipid/DNA arrangement, we have to argue against the notion that the heterogeneity of the film observed optically is due to laterally segregated lattices of lipid and DNA. This is done as follows: The lipid lattices in the presence and absence of DNA were found structurally different. Hence, there is at least some DNA under the lipid lattice. Still this DNA fraction may not diffract, and we might measure diffraction from DNA in the continuous phase. However, this phase is reduced in area fraction upon compression. In contrast, we observe an increase of the integrated X-ray intensity by a factor of 3. Making a rough estimate, assuming all lipids in the ordered phase with, according to X-ray data, a molecular area of 60 Å^2/molecule, which within 5% is independent of pressure. Compression from a molecular area of 150 to 80 Å^2/molecule (see isotherm, Figure 1) increases the lipid/area fraction from $^2/_5$ to $^3/_4$, i.e., about a factor of 2; the other fraction would decrease by a factor of 2.5. Hence, the majority of the intensity increase may be ascribed to the increase in area fraction of the lipid phase coupled with DNA, and the remaining deviation could be the result of a change in Debye−Waller factor. This is especially true for the intensity decrease on increasing the pressure above 30 mN/m. Since the above arguments would suggest an intensity increase, we have to argue in favor of weaker lateral coupling at higher pressures increasing the Debye−Waller factor.

Consequently, the data are consistent with the model of rodlike DNA forming a one-dimensional lattice under a hexagonal or distorted hexagonal (centered rectangular) lattice although the correlation lengths are only on the order of 100 Å (Figure 6). A similar size of the DNA domains (near 10 neighboring chains) was reported by Safinya et al.[24,38] for DNA bound in lamellar structures. Our data give no information about the extension of order in the direction parallel to the DNA strands, but the persistence length of native DNA of about 600 Å[26] allows the assumption that the order can be maintained over possibly a few hundred angstroms. No information can be given about hypothetical effects of the direction of compression to a preferred main direction of DNA alignment. The incoming X-ray beam is in fixed orientation perpendicular to the direction of compression. Both the lipid and the DNA lattice cannot be correlated to each other in terms of planar inhomogeneity. On compression, the lateral density of condensed lipid increased by less than 5% whereas the DNA density can increase by almost 40%. Hence, we cannot expect any matching of the two lattices in general. Still there might be commensurability into one lattice direction if a repeat distance along the DNA rod (34 Å per helix) was an integer multiple of a lipid spacing. This cannot be ruled out since 34 Å/7 = 4.86 Å is close to the lattice spacing a, but the coupling would then be very weak because the spacing a changes with pressure. Also, a one-dimensional lattice coupling to a hexagonal one is breaking its symmetry and thus distorting it in contrast to the finding at 20 mN/m. The latter would also hold if there is no commensurability but merely epitaxy. Hence, these influences are too weak, probably due to smearing of charges along the DNA backbone.

It is very difficult to understand the higher compressibility of the DNA lattice compared to the lipid lattice, measured by diffraction. This can be explained assuming some fraction of disordered areas with higher compressibility in between those ordered domains seen by BAM. Figure 7 pictures the model of this proposed coexistence, which is the most likely one after taking the inhomogeneous pictures of BAM and AFM into account. Domains of this kind have also been observed by AFM for polyethylenimine coupled to fatty acid monolayers.

We should also note that these results are at variance with measurements on the synthetic (stiff) polyelectrolyte PDADMAC coupled to oppositely charged phospholipid monolayers.[39] There, although the polymer−polymer spacings could not be measured, a polymer alignment with commensurability into one direction could be deduced. The polyelectrolyte coupling enforced an almost pressure-independent aliphatic chain tilt, and this may be attributed to the smaller dimension of PDADMAC enabling denser lateral packing.

In conclusion, we have shown that DNA coupling to an otherwise liquid membrane surface condenses this locally and itself forms a nematic alignment. DNA and lipid density are interrelated, but not in a straightfor-

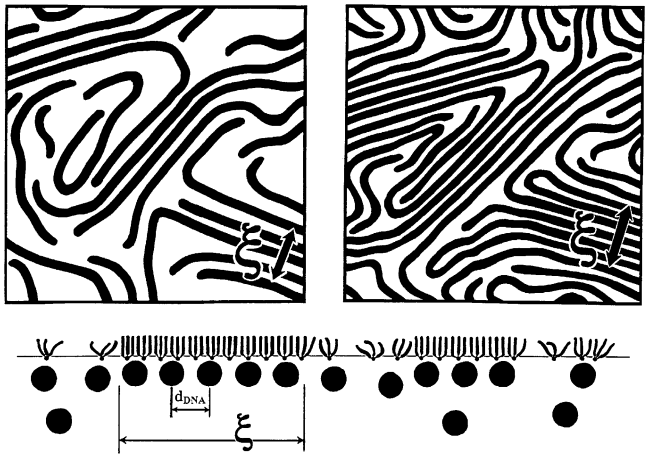

Figure 7. Model of the most likely structure of DNA coupled to a TODAB monolayer, showing two top views of the DNA layer (without lipid molecules) before and after compression. The increase of the correlation length ξ is not due to more DNA molecules reaching the surface but to formerly disordered DNA strands that arrange parallel to the ordered domains. A vertical cut in the lower sketch shows the cross section of the DNA arranged in a regular distance d_{DNA}. The order is lost at the edges of the domains with the correlation length ξ. The hydrocarbon chains of the TODAB molecules are more condensed when coupled to DNA. The structure of the less ordered gaps in between is not characterized experimentally.

ward way like lattice commensurability. Instead, there is a delicate interplay of lateral and normal DNA interactions that are now open for dedicated measurements to understand processes like nonviral transfection and diagnostics.

Acknowledgment. This work was supported by the Deutsche Forschungsgemeinschaft. We thank HASYLAB (DESY, Hamburg, Germany) for providing beamtime and Kristian Kjaer (Risoe, Denmark) for his excellent work to keep the liquid surface spectrometer at BW1 running in a very high quality.

References and Notes

(1) Miller, A. D. *Angew. Chem.* **1998**, *110*, 1862.
(2) Lasic, D. D.; Papahadjopoulos, D. *Curr. Opin. Solid State Mater. Sci.* **1996**, *1*, 392.
(3) Dass, C. R. *J. Cancer Res. Clin. Oncol.* **2002**, *128*, 177.
(4) Ferrari, M. E.; Rusalov, D.; Enas, J.; Wheeler, C. J. *Nucleic Acids Res.* **2002**, *30*, 1808.
(5) Ilies, M. A.; Balaban, A. T. *Expert Opin. Ther. Patents* **2001**, *11*, 1729.
(6) Carriere, M.; Trunchant, I.; Niore, P.; Byk, G.; Mignet, N.; Escriou, V.; Scherman, D.; Herscovici, J. *J. Liposome Res.* **2002**, *12*, 95.
(7) Xu, Y.; Szoka, F. C. *Biochemistry* **1996**, *35*, 5616.
(8) Crystal, R. G. *Science* **1995**, *270*, 404.
(9) Sastry, M.; Ramakrishnan, V.; Pattarkine, M.; Gole, A.; Ganesh, K. N. *Langmuir* **2000**, *16*, 9142.
(10) Chee, M.; Yang, R.; Hubbell, E.; Berno, A.; Huang, X. C.; Stern, D.; Winkler, J.; Lockhart, D. J.; Morris, M. S.; Fodor, S. P. A. *Science* **1996**, *274*, 610.
(11) Bensimon, A.; Simon, A.; Chiffaudel, A.; Croquette, V.; Heslot, F.; Bensimon, D. *Science* **1994**, *265*, 2096.
(12) Fukushima, T.; Inoue, Y.; Hayakawa, T.; Taniguchi, K.; Miyazaki, K.; Okahata, Y. *J. Dent. Res.* **2001**, *80*, 1772.
(13) Brown, M. D.; Schätzlein, A. G.; Uchegbu, I. F. *Int. J. Pharm.* **2001**, *229*, 1.
(14) Ruiz, F. E.; Clancy, J. P.; Perricone, M. A. *Hum. Genet. Ther.* **2001**, *12*, 751.
(15) Spack, E. G.; Sorgi, F. L. *Drug Discov. Today* **2001**, *6*, 186.
(16) Barenholz, Y. *Curr. Opin. Colloid Interface Sci.* **2001**, *6*, 66.
(17) Zabner, J.; Fasbender, A. J.; Moninger, T.; Poellinger, K. A.; Welsh, M. J. *J. Biol. Chem.* **1995**, *270*, 18997.
(18) Woodle, M. C.; Scaria, P. *Curr. Opin. Colloid Interface Sci.* **2001**, *6*, 78.
(19) Francescangeli, O.; Stanic, V.; Gobbi, L.; Bruni, P.; Iacussi, M.; Tosi, G.; Bernstorff, G. *Phys. Rev. E* **2003**, *67*, 1.
(20) Caracciolo, C.; Caminiti, R.; Pozzi, D.; Friello, M.; Boffi, F.; Castellano, A. C. *Chem. Phys. Lett.* **2002**, *351*, 222.
(21) Zantl, R.; Baicu, L.; Artzner, F.; Sprenger, I.; Rapp, G.; Rädler, J. O. *J. Phys. Chem. B* **1999**, *103*, 10300.
(22) Salditt, T.; Koltover, I.; Rädler, J. O.; Safinya, C. R. *Phys. Rev. Lett.* **1997**, *79*, 2582.
(23) Rädler, J. O.; Koltover, I.; Salditt, T.; Safinya, C. R. *Science* **1997**, *275*, 810.
(24) Safinya, C. R.; Koltover, I.; Rädler, J. *Curr. Opin. Colloid Interface Sci.* **1998**, *3*, 69.
(25) Rädler, J. O.; Koltover, I.; Jamieson, A.; Salditt, T.; Safinya, C. R. *Langmuir* **1998**, *14*, 4272.
(26) Podgornik, R.; Rau, D. C.; Parsegian, V. A *Macromolecules* **1989**, *22*, 1780.
(27) Leonenko, Z. V.; Merkle, D.; Lees-Miller, S. P.; Cramb, D. T. *Langmuir* **2002**, *18*, 4873.
(28) Fang, Y.; Yang, Y. *J. Phys. Chem. B* **1997**, *101*, 441.
(29) Cai, X.; Yang, J. *Biophys. J.* **2002**, *82*, 357.
(30) Pfohl, T.; Li, Y.; Wen, Z.; Wong, G. C. L.; Koltover, I.; Kim, M. W.; Safinya, C. R. *Colloids Surf. A: Physicochem. Eng. Aspects* **2001**, *198−200*, 613.
(31) Wong, G. C. L.; Li, Y.; Koltover, I.; Safinya, C. R. *Appl. Phys. Lett.* **1998**, *73*, 2042.
(32) Schindler, T.; Nordmeier, E. *Macromol. Chem. Phys.* **1997**, *198*, 1943.
(33) Frahm, R.; Weigelt, J.; Meyer, G.; Materlik, G. *Rev. Sci. Instrum.* **1995**, *66*, 1677.
(34) Kjaer, K. *Physica B* **1994**, *198*, 100.
(35) Schneider, M.; Brinkmann, M.; Möhwald, H. *Macromolecules* **2003**, *36*, 9510.
(36) Netz, R. R. *Phys. J.* **2002**, *1*, 51.
(37) Netz, R. R.; Joanny, J.-F. *Macromolecules* **1999**, *32*, 9013.
(38) Salditt, T.; Koltover, I.; Rädler, J. O.; Safinya, C. R. *Phys. Rev. E* **1998**, *58*, 889.
(39) de Meijere, K.; Brezesinski, G.; Möhwald, H. *Macromolecules* **1997**, *30*, 2337.

MA0348425